Acta Crystallographica Section B
Structural Science
ISSN 0108-7681

Role of strong intramolecular N—H···N hydrogen bonds in determining the conformation of adenosine-receptor antagonists

Valeria Ferretti,[a]* Loretta Pretto,[a] Mojgan Aghazadeh Tabrizi[b] and Paola Gilli[a]

[a]Dipartimento di Chimica and Centro di Strutturistica Diffrattometrica, University of Ferrara, via L. Borsari 46, I-44100 Ferrara, Italy, and [b]Dipartimento di Scienze Farmaceutiche, University of Ferrara, via Fossato di Mortara 17-19, I-44100 Ferrara, Italy

Correspondence e-mail: frt@unife.it

Received 20 January 2006
Accepted 18 April 2006

Over the last few years many efforts have been devoted to the discovery of new adenosine antagonists which can selectively bind to one of the four adenosine receptors, called A_1, A_{2A}, A_{2B} and A_3, in order to develop new drugs with few side effects. The present paper reports the crystal structures of four newly synthesized antagonists belonging to the chemical class of pyrazolo-triazolo-pyrimidine derivatives, which display good affinity and selectivity properties towards the A_{2A} or A_3 receptor subtypes. These molecules assume an overall planar conformation due to the formation of strong intramolecular N—H···N hydrogen bonds. A systematic investigation on molecules containing the ureidic —NH—C(=O,S)—NH—C=N— fragment has shown that the formation of such interactions is a common feature for this class of compounds. The associated energy, evaluated through DFT calculations, is some 50.24 kJ mol^{-1}, leading to the conclusion that the hydrogen bond, and consequently the planar conformation, is retained not only in the solid state but also in solution during the interaction of the molecule with its receptor.

1. Introduction

Adenosine is the endogenous ligand of four receptors, called A_1, A_{2A}, A_{2B} and A_3, which display different pharmacological profiles and tissue distribution. When bound to one of its receptors, it is responsible for a variety of effects, such as the general depression of the central nervous system activity, vasodilation and inhibition of platelet aggregation (Jarvis & Williams, 1987). In connection with the diverse physiological functions of adenosine, a vast amount of effort is being invested in developing new pharmacological tools or potential drugs which act at adenosine receptors; however, the use of agonists and antagonists acting on the adenosine system gives rise to numerous side effects which are caused by the presence of a high number of action sites throughout the body and the lack of tissue or receptor selectivity. For these reasons, in the last few years many efforts have been devoted to find adenosine agonists or antagonists with enhanced selectivity properties able to preferentially bind to one of the four receptor subtypes. In particular, selective adenosine antagonists could be used in the therapeutic treatment of cognitive deficit, renal failure and cardiac arrhythmias (A_1 antagonists; Müller, 1997), in the cure of Parkinson's disease (A_{2A} antagonists; Richardson *et al.*, 1997) or asthma and other inflammatory processes (A_{2B} and A_3 antagonists; Jacobson, 1998).

While all the selective and potent agonists designed so far belong to the chemical class of the adenosine derivatives, the antagonists can be chemically very different, being, for

Table 1
Experimental details.

	(1)	(2)	(3)	(4)
Crystal data				
Chemical formula	$C_{18}H_{13}O_2N_8Cl\cdot0.5H_2O$	$C_{22}H_{22}N_8O_3$	$C_{22}H_{22}N_8O_3\cdot0.5C_4H_8O_2$	$C_{20}H_{18}N_8SO_3\cdot H_2O$
M_r	417.82	446.48	490.53	468.50
Cell setting, space group	Triclinic, $P\overline{1}$	Monoclinic, $P2_1/c$	Triclinic, $P\overline{1}$	Triclinic, $P\overline{1}$
a, b, c (Å)	6.9825 (1), 15.7877 (3), 17.8780 (4)	11.2816 (2), 24.0888 (5), 8.1651 (3)	12.6218 (2), 14.0932 (3), 15.6948 (4)	10.1490 (3), 10.5112 (3), 11.4025 (4)
α, β, γ (°)	100.2320 (9), 95.906 (1), 100.567 (1)	90.00, 103.9170 (8), 90.00	72.8670 (7), 71.3280 (7), 70.6350 (9)	110.1850 (18), 97.9640 (18), 99.6510 (13)
V (Å^3)	1887.81 (6)	2153.81 (10)	2439.16 (9)	1099.89 (6)
Z	4	4	4	2
D_x (Mg m^{-3})	1.470	1.377	1.336	1.415
Radiation type	Mo $K\alpha$	Mo $K\alpha$	Mo $K\alpha$	Mo $K\alpha$
No. of reflections for cell parameters	14 447	9542	15 610	10 025
θ range (°)	3.4–28.0	2.7–28.0	2.0–27.0	1.0–30.0
μ (mm^{-1})	0.24	0.10	0.10	0.19
Temperature (K)	295	295	295	295
Crystal form, colour	Plate, colourless	Plate, colourless	Prism, colourless	Plate, colourless
Crystal size (mm)	0.50 × 0.38 × 0.12	0.51 × 0.19 × 0.07	0.33 × 0.24 × 0.19	0.50 × 0.28 × 0.05
Data collection				
Diffractometer	Nonius Kappa CCD	Nonius Kappa CCD	Nonius Kappa CCD	Nonius Kappa CCD
Data collection method	φ and ω scans	φ and ω scans	φ and ω scans	φ and ω scans
Absorption correction	None	None	None	None
No. of measured, independent and observed reflections	14 447, 8951, 6646	9542, 5159, 2594	15 610, 10 558, 6467	10 025, 4777, 2970
Criterion for observed reflections	$I > 2\sigma(I)$	$I > 2\sigma(I)$	$I > 2\sigma(I)$	$I > 2\sigma(I)$
R_{int}	0.022	0.057	0.024	0.028
θ_{max} (°)	28.0	28.0	27.0	27.0
Range of h, k, l	$-9 \Rightarrow h \Rightarrow 9$ $-20 \Rightarrow k \Rightarrow 20$ $-23 \Rightarrow l \Rightarrow 20$	$-14 \Rightarrow h \Rightarrow 14$ $-30 \Rightarrow k \Rightarrow 31$ $-10 \Rightarrow l \Rightarrow 10$	$-13 \Rightarrow h \Rightarrow 16$ $-17 \Rightarrow k \Rightarrow 17$ $-19 \Rightarrow l \Rightarrow 20$	$-12 \Rightarrow h \Rightarrow 12$ $-13 \Rightarrow k \Rightarrow 13$ $-14 \Rightarrow l \Rightarrow 14$
Refinement				
Refinement on	F^2	F^2	F^2	F^2
$R[F^2 > 2\sigma(F^2)]$, $wR(F^2)$, S	0.048, 0.138, 1.06	0.060, 0.141, 1.02	0.061, 0.183, 1.04	0.058, 0.196, 1.11
No. of reflections	8951	5159	10 558	4777
No. of parameters	644	396	889	381
H-atom treatment	Refined independently	Refined independently	Mixture of independent and constrained refinement	Mixture of independent and constrained refinement
Weighting scheme	$w = 1/[\sigma^2(F_o^2) + (0.0603P)^2 + 0.4454P]$, where $P = (F_o^2 + 2F_c^2)/3$	$w = 1/[\sigma^2(F_o^2) + (0.0509P)^2 + 0.3032P]$, where $P = (F_o^2 + 2F_c^2)/3$	$w = 1/[\sigma^2(F_o^2) + (0.0836P)^2 + 0.5314P]$, where $P = (F_o^2 + 2F_c^2)/3$	$w = 1/[\sigma^2(F_o^2) + (0.0858P)^2 + 0.3977P]$, where $P = (F_o^2 + 2F_c^2)/3$
$(\Delta/\sigma)_{max}$	0.004	0.001	0.001	0.001
$\Delta\rho_{max}$, $\Delta\rho_{min}$ (e Å^{-3})	0.24, −0.39	0.19, −0.24	0.27, −0.20	0.53, −0.24
Extinction method	None	None	*SHELXL*	None
Extinction coefficient	–	–	0.054 (5)	–

Computer programs used: *Kappa CCD server software* (Nonius, 1997), *DENZO-SMN* (Otwinowski & Minor, 1997), *SIR*97 (Altomare *et al.*, 1999), *SHELXL*97 (Sheldrick, 1997), *ORTEP*III (Burnett & Johnson, 1996), *PARST* (Nardelli, 1995), *WINGX* (Farrugia, 1999).

example, xanthinic (Kim *et al.*, 2000, 2002; Hayallah *et al.*, 2002; Baraldi *et al.*, 2004), xanthiene (Berk *et al.*, 2006) or pyrazolo derivatives (Kim *et al.*, 1998; Baraldi *et al.*, 2002, 2005; Fossa *et al.*, 2005). The measure of the binding constants of all these new synthesized molecules has led to extensive structure–activity relationship studies, which highlight the key structural features of agonists and antagonists required for receptor affinity and subtype selectivity (Colotta *et al.*, 2000; Hess *et al.*, 2000; Baraldi *et al.*, 2002; Gao *et al.*, 2002) in an attempt to map the binding site of any specific receptor. The structures of adenosine receptors are still unknown, even though some information on the binding domains has been obtained by recent site-mutagenesis studies (Fredholm *et al.*, 2001) aimed at identifying the aminoacidic residues involved in the molecule–macromolecule interactions.

We present here the crystal structures of four antagonists, sketched in (I), belonging to the chemical class of the pyrazolo-triazolo-pyrimidines, which exhibit good affinity and selectivity properties towards the A_3 [compounds (1)–(3)] or A_{2A} [compound (4)] receptor subtypes. All four present a

Table 2
Experimental bond lengths for (1)–(4), mean values for molecules retrieved from the CSD and DFT-calculated values for the two sample molecules of Scheme (III) in their *closed* conformation (Å).

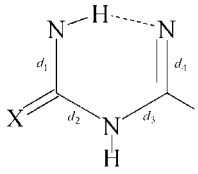

							DFT	
	(1)	(2)	(3)	(4)	CSD (X = O)	CSD (X = S)	Calc.(*a*)	Calc.(*b*)
d_1	1.352 (2)	1.341 (3)	1.336 (3)	1.333 (6)	1.34 [2]	1.33 [1]	1.363	1.361
	1.351 (2)		1.340 (3)					
d_2	1.405 (2)	1.411 (3)	1.406 (3)	1.403 (6)	1.39 [2]	1.37 [1]	1.422	1.430
	1.399 (2)		1.401 (3)					
d_3	1.365 (3)	1.360 (3)	1.364 (4)	1.370 (5)	1.38 [1]	1.40 [1]	1.375	1.362
	1.366 (2)		1.357 (4)					
d_4	1.293 (2)	1.295 (3)	1.291 (3)	1.290 (5)	1.33 [2]	1.33 [1]	1.348	1.307
	1.296 (2)		1.293 (3)					
C═X	1.213 (2)	1.214 (3)	1.214 (4)	1.225 (5)	1.23 [1]	1.68 [1]	1.228	1.226
	1.219 (2)		1.217 (4)					
Hydrogen-bond parameters								
N···N	2.682 (2)	2.725 (3)	2.697 (3)	2.721 (5)	2.68 [3]	2.65 [2]	2.731	2.746
	2.653 (2)		2.722 (3)					

peculiar structural characteristic, *i.e.* the formation of remarkably strong intramolecular N—H···N hydrogen bonds which are able to increase the rigidity of the molecules conferring on them an overall planarity.

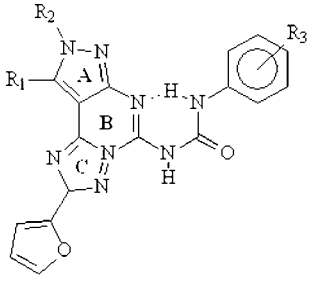

1: R_1=H: R_2= Me; R_3= *o*-Cl
2: R_1=H: R_2= Bu; R_3= *m*-OMe
3: R_1=H: R_2= Bu; R_3= *o*-OMe
4: R_1=SMe: R_2= Me; R_3= *p*-OMe

(I)

Extensive studies carried out on homonuclear and heteronuclear O—H···O and N—H···O bonds (Gilli *et al.*, 1994, 2000) have shown that hydrogen bonds of strength comparable with those presently considered can occur in neutral molecules only when the donor and acceptor atoms are connected by a π-conjugated system, in such a way as to establish a synergistic interplay between the π-delocalization of the conjugated fragment and hydrogen-bond strengthening (RAHB = resonance-assisted hydrogen bond model). The present compounds, however, do not fit in any way the classical RAHB model, giving the problem of which other factors could strengthen the N—H···N bond by inducing partial charges of the correct sign on the donor and acceptor atoms. It will be shown that the present findings can be interpreted in the frame of the *PA/pKa equalization rule*, a general model used for interpreting the strength of all hydrogen bonds (including RAHBs; Gilli *et al.*, 2002, 2004, 2005) and based on the hypothesis that such a strength is determined by the differences of the proton affinities (ΔPA) or acid–base dissociation constants (ΔpK_a) of the hydrogen-bond donor and acceptor groups, the hydrogen bond being stronger when these differences are smaller.

A CSD (Allen *et al.*, 1979) search and DFT calculations have been performed, to verify that this new type of strong hydrogen bond is a common feature of the compounds containing the —N═C—NH—C(═*X*)—NH— fragment and that the energy associated with its formation is high enough to also maintain the planar conformation in solution, and consequently during the interaction with the receptor.

2. Experimental and computational methods

The synthesis and biological data of the four molecules: *N*-[8-methyl-2-(2-furyl)-8*H*-pyrazolo[4,3-*e*][1,2,4]triazolo[1,5-c]pyrimidin-5-yl]-*N*′-(2-chlorophenyl)urea (1); *N*-[8-butyl-2-(2-furyl)-8*H*-pyrazolo[4,3-*e*][1,2,4]triazolo[1,5-*c*]pyrimidin-5-yl]-*N*′-(3-methoxyphenyl)urea (2); *N*-[8-butyl-2-(2-furyl)-8*H*-pyrazolo[4,3-*e*][1,2,4]triazolo[1,5-*c*]pyrimidin-5-yl]-*N*′-(2-methoxyphenyl)urea (3) and *N*-[8-methyl-2-(2-furyl)-9-(methylthio)-8*H*-pyrazolo[4,3-*e*][1,2,4]triazolo[1,5-*c*]pyrimidin-5-yl]-*N*′-(4-methoxyphenyl)urea hydrate (4) have been reported elsewhere (Baraldi *et al.*, 2000, 2003). Suitable crystals were obtained by slow evaporation at room temperature from a mixture of hot methanol and 1,4 dioxane [(1) and (3)], dimethylformamide and 1,4 dioxane [(2)], and acetone and acetonitrile [(4)]. Crystal data, data collection and refinement parameters are summarized in Table 1[1] and a selection of bond lengths and angles is reported in Table 2. X-ray diffraction data were collected on a Nonius Kappa CCD diffractometer using graphite-monochromated Mo $K\alpha$ radiation (λ = 0.71069 Å). Intensities were corrected for Lorentz and polarization effects. The structures were solved by direct methods with the *SIR*97 program (Altomare *et al.*, 1999) and refined by full-matrix least squares using the *SHELXL*97 (Sheldrick, 1997) program. For all compounds non-H atoms were refined anisotropically and H atoms isotropically, with the exception of H atoms belonging to the disordered parts, which were

[1] Supplementary data for this paper are available from the IUCr electronic archives (Reference: DE5026). Services for accessing these data are described at the back of the journal.

included in calculated positions, riding on the attached atoms. In (3) and (4) the positions of the H atoms belonging to the solvent molecules were not included in the refinement. All other calculations were performed using the programs *WinGX* (Farrugia, 1999) and *PARST* (Nardelli, 1995). Hydrogen-bonding parameters for the four structures, including those for C—H···*X* bonds, are reported in Table 3. In general, we have considered the C—H···*X* (*X* = N,O) interactions where the H···*X* distance is less than 2.70 Å and the C—H···*X* angle is greater than 130° to be significant.

A total of 36 and 68 structures containing the fragment of Scheme (II) with *X* = O and S, respectively, has been retrieved from the Cambridge Structural Database (April 2005 version). Structures of low quality ($R > 0.10$), that are disordered or in which the positions of the H atoms have not been determined, were excluded.

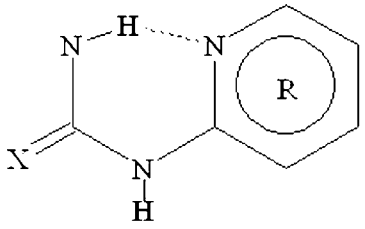

R = any aromatic ring

(II)

Quantum-mechanical calculations have been performed on the two test molecules (*a*) and (*b*) of Scheme (III), with the aim of evaluating the hydrogen-bond energy, ΔE_{HB}, calculated as the difference in energy between two conformations: the '*closed*' conformation (*i.e.* where the hydrogen bond is present) and the '*open*' one (*i.e.* without any intramolecular hydrogen bond). The problem of choosing an appropriate level of theory for strong hydrogen bonds has been widely investigated by several authors (Frisch *et al.*, 1985; Barone & Adamo, 1996; Buemi & Zuccarello, 1996; Chung *et al.*, 1997; Kobko *et al.*, 2001). It is generally recognized that the hydrogen-bond geometry cannot be reproduced at the Hartree–Fock level and that electron correlation can be satisfactorily accounted for both by *ab initio* MP2 (or higher) methods and by density functional theory (DFT) methods with a proper functional. In view of these considerations and of the fact that DFT methods are faster, all calculations were performed by using the Dmol^3 code of the *MaterialStudio* system of programs (Accelrys Inc., 2003), in the framework of the Perdew—Wang generalized-gradient approximation (PW91; Perdew & Wang, 1992). The geometry optimization of the open and closed conformations has been performed by using the numeric DNP basis set, which, although comparable to the 6-31G** Gaussian basis set, is believed to be more accurate. Some selected calculated geometrical parameters are reported in Table 2.

Table 3
Hydrogen-bonding parameters (Å, °).

	D—H	*D*···*A*	H···*A*	*D*—H···*A*
(1)				
N1*A*—H···N3*A*	0.92 (2)	2.682 (2)	1.90 (2)	141 (2)
N2*A*—H···O1*B*	0.85 (2)	2.841 (2)	2.04 (2)	158 (2)
N1*B*—H···N3*B*	0.87 (3)	2.653 (2)	1.91 (3)	142 (2)
N2*B*—H···O1*A*	0.82 (2)	2.946 (2)	2.16 (2)	161 (2)
O1*W*—H1*W*···N6*A*	1.05 (5)	2.871 (4)	1.85 (5)	161 (4)
O1*W*—H2*W*···O1*W*^{i}	0.90 (5)	3.026 (6)	2.51 (5)	117 (4)
C10*B*—H1···O2*A*^{ii}	1.01 (3)	3.467 (3)	2.49 (3)	162 (2)
C18*B*—H1···N8*A*^{ii}	0.94 (4)	3.479 (4)	2.64 (4)	149 (3)
C17*B*—H1···O1*W*^{iii}	0.97 (4)	3.446 (5)	2.48 (4)	171 (3)
(2)				
N1—H1···N3	0.89 (3)	2.725 (3)	1.98 (3)	140 (2)
C10—H1···O3^{iv}	0.98 (2)	3.239 (3)	2.28 (2)	167 (2)
C20—H···N4^{v}	0.99 (2)	3.505 (3)	2.64 (2)	145 (2)
C18—H1···N6^{vi}	1.01 (4)	3.619 (4)	2.61 (4)	172 (3)
C17—H1···N7^{vii}	1.03 (4)	3.664 (4)	2.64 (4)	172 (3)
(3)				
N1*A*—H···N3*A*	0.87 (3)	2.697 (3)	1.96 (3)	142 (3)
N1*B*—H···N3*B*	0.86 (3)	2.722 (3)	1.98 (3)	143 (2)
C10*B*—H···O60*A*	0.96 (3)	3.14 (1)	2.24 (3)	157 (2)
C10*A*—H1···O50^{viii}	0.98 (3)	3.417 (7)	2.46 (3)	166 (2)
C17*A*—H1···O1*B*^{ix}	0.93 (4)	3.400 (5)	2.49 (4)	166 (3)
C4*A*—H1···O2*B*^{x}	0.98 (4)	3.449 (4)	2.63 (4)	142 (2)
C5*A*—H···N8*B*^{x}	1.06 (4)	3.729 (4)	2.68 (4)	169 (3)
C17*B*—H1···O1*A*^{xi}	0.94 (7)	3.30 (5)	2.41 (5)	160 (4)
(4)				
N1—H···N3	0.81 (5)	2.724 (4)	2.08 (5)	136 (4)
N2—H···O2*A*	0.77 (3)	3.061 (8)	2.45 (3)	136 (3)
O1*A*—H1···O1	0.86	3.002 (5)	2.17	164
O2*A*—H1···O1*A*	0.83	2.63 (1)	2.02	129
C20—H1···N6	0.97 (5)	3.422 (6)	2.56 (5)	148 (4)
O1*A*—H2···N4^{xii}	0.95	2.847 (7)	1.92	163
O2*A*—H2···O1*A*^{xiii}	1.03	2.768 (8)	1.86	147
C20—H2···O2*A*^{xiv}	1.00 (4)	3.484 (7)	2.63 (3)	143 (3)

Symmetry codes: (i) $2-x,-y-1,-z$; (ii) $2-x,-y,-z-1$; (iii) $2-x,-y,-z$; (iv) $-x,\frac{1}{2}+y,\frac{3}{2}-z$; (v) $x,\frac{1}{2}-y,\frac{1}{2}+z$; (vi) $-x,y-\frac{1}{2},\frac{3}{2}-z$; (vii) $-x-1,-y,2-z$; (viii) $2-x,-y,-z$; (ix) $x,y,1+z$; (x) $x+1,y,z$; (xi) $x-1,y,z$; (xii) $1-x,1-y,-z$; (xiii) $-x,1-y,-z$; (xiv) $1-x,1-y,1-z$.

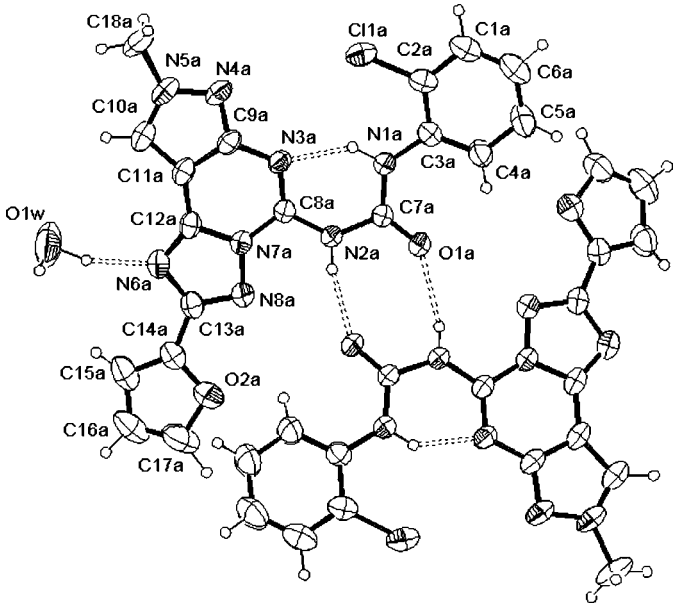

Figure 1
*ORTEP*III (Burnett & Johnson, 1996) view and atom numbering for (1). The displacement ellipsoids are drawn at 40% probability.

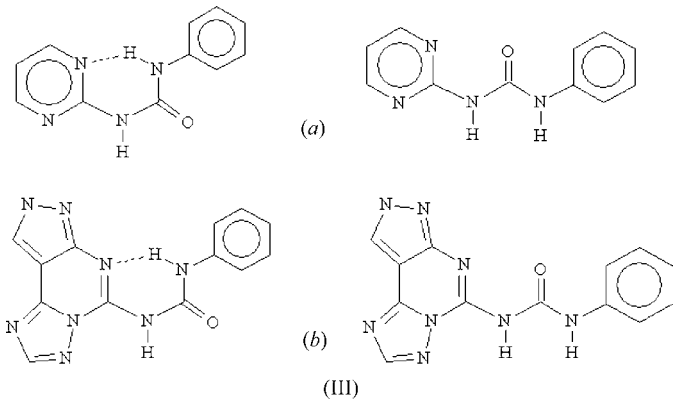

(III)

3. Results and discussion

*ORTEP*III (Burnett & Johnson, 1996) views of (1)–(4) are shown in Figs. 1–4. All the molecules are remarkably flat, the planarity being due not only to the presence of fused aromatic rings (angles between the calculated mean-square planes for *A*, *B* and *C* rings are in the range 0.4–8.8°), but also to the presence of an intramolecular N—H···N hydrogen bond involving the ureidic moiety and closing a further six-membered ring whose geometrical parameters, reported in Table 2, are remarkably similar in all the molecules.

The structural parameters of the NH/OH···O/N and CH···O/N intermolecular interactions involved in crystal formation are reported in Table 3. The asymmetric unit of (1) consists of two molecules, forming a dimeric pair *via* N2—H···O1 hydrogen bonds, and of one co-crystallized water molecule. Two dimers are in turn connected in chains by N6*A*···H_2O···H_2O···N6*A* hydrogen bonding, as reported in Table 3. In (2) the lateral part (C5—H) of the phenyl ring bonded to N1 is disordered over two non-equivalent positions. Here the crystal architecture is built up mainly by C—H···*X* weak interactions, probably because the presence of the bulky buthyl group on ring *A* and the methoxy group on the N1 phenyl substituent makes the approach of the molecules difficult, hindering the formation of hydrogen-bonded dimers or chains. The asymmetric unit of (3) is rather complicated,

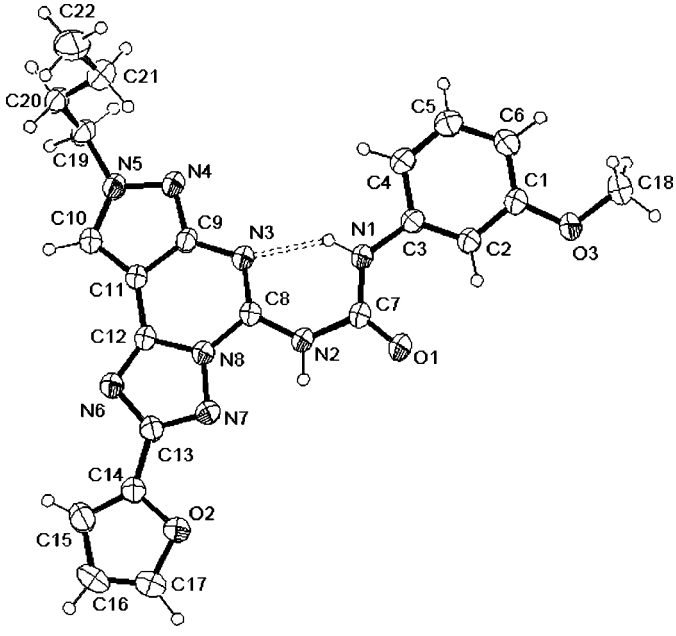

Figure 2
*ORTEP*III (Burnett & Johnson, 1996) view and atom numbering for (2). The displacement ellipsoids are drawn at 40% probability.

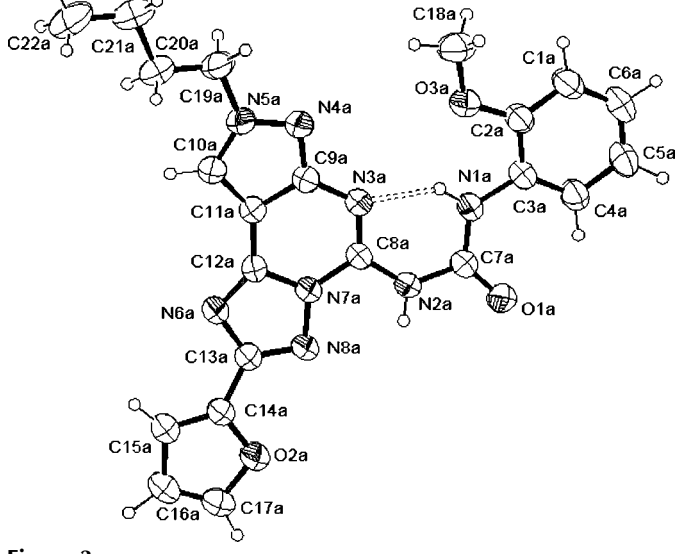

Figure 3
*ORTEP*III (Burnett & Johnson, 1996) view and atom numbering for (3). The displacement ellipsoids are drawn at 40% probability. For the sake of clarity, only one molecule of the asymmetric unit is shown and the solvent molecules are omitted.

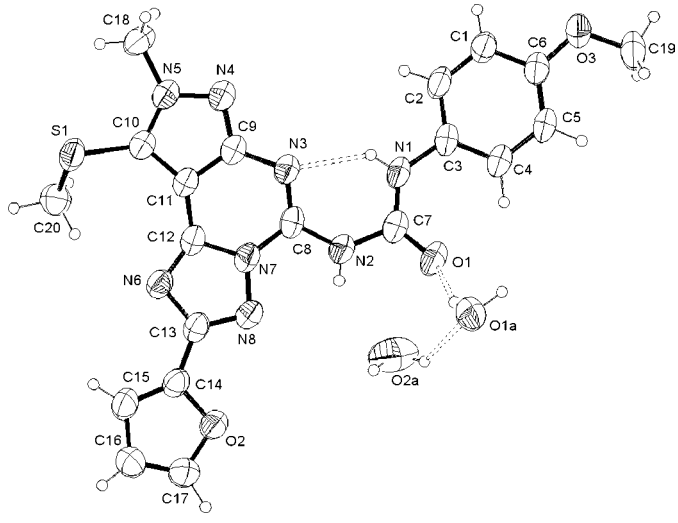

Figure 4
*ORTEP*III (Burnett & Johnson, 1996) view and atom numbering for (4). The displacement ellipsoids are drawn at 40% probability.

being formed by molecules of triazolo-pyrazolo-pyrimidine derivatives [(1) in Scheme (I)] and 1,4 dioxane in a 2:1 ratio (two solvent molecules are positioned on symmetry centers). The dioxane molecules are disordered, being present inside the crystal in the two energetically equivalent chair conformations; the furane moiety of molecule *B* is also disordered. The hydrogen-bond acceptor atoms, in particular the carbonyl and the dioxane O atoms, are involved in C—H···O interactions. The asymmetric unit of (4) includes one drug molecule and one water molecule, disordered over two equivalent positions, whose H atoms have been found in the difference Fourier map but kept fixed during the refinement. The disordered water is linked with its centrosymmetrically related molecule forming a square, and connecting two drug molecules of different asymmetric units by O—H···N4 and O—H···O1 interactions. The result is a complicated three-dimensional network.

All four molecules are characterized by the presence of a rather strong intramolecular N1—H···N3 hydrogen bond, whose N···N distances range from 2.653 (2) to 2.725 (3) Å. The hydrogen-bond occurrences in compounds containing the fragment of Scheme (II) have been reviewed through a systematic CSD investigation. For each structure, d_1–d_4 [see Scheme (IV)] and C═*X* bond distances together with hydrogen-bond parameters have been considered and their mean values are reported in Table 2. All N—N distances are reported in Fig. 5 as separate histograms for the two classes of compounds with *X* = O and *X* = S; here the positions occupied by the N—N values of (1)–(4) are marked by arrows.

(I) (II)

(IV)

Comparison of the bond distances d_1–d_4 of Table 2 shows that the geometry of the fragment involved in the hydrogen-bond formation is substantially conserved, apart from the d_4 value that in (1)–(4) is shorter than the mean value derived from the CSD search. This discrepancy is ascribable to the fact that in our CSD search d_4 is part of an aromatic ring, while in the present structures such a distance has a more marked double-bond character.

The mean N—N distances are 2.68 (3) and 2.65 (2) Å for structures with *X* = O and *X* = S, respectively. These values are significantly shorter than those found for non-resonant N—H···N bonds, which range from 2.70 to 3.30 Å with a mean value of ∼3.0 Å, which are in perfect agreement with those found in typical N—H···N RAHBs (range: 2.50–2.88 Å) depicted in (I) of Scheme (IV) (Gilli, Fernàndez-Castaño *et al.*, 1996). Here the resonance induces an electron shifting in the hydrogen-bonded six-membered ring so that the donor and acceptor atoms can acquire partial charges having the correct sign to strengthen the hydrogen bond itself. The rather different delocalization pattern found in the present molecules, sketched in (II) of Scheme (IV), does not meet RAHB requirements because the alternation of simple and double bonds within the ring is interrupted by the single bond d_2. The π-conjugation process within the two occurring S/O═C—NH and N—C═N groups, nevertheless, appears to be able to redistribute the partial charges on the donor and acceptor atoms in such a way to reproduce the same result found in (I) shown in Scheme (IV).

The strength of the N—H···N hydrogen bond can than be explained by directly applying the '*pK_a equalization rule*' (Gilli *et al.*, 2002, 2004, 2005). The fragment (II) can be regarded as constituted by two moieties: an O═C—NH— amidic part (hydrogen-bond donor) and a N═C—NH— amidinic one (hydrogen-bond acceptor). Such an amide/amidine couple is quite able to satisfy the necessary condition of pK_a matching or the formation of strong hydrogen bonds since their pK_a values are very similar, being in the ranges 15–17 and 12–14, respectively (Maskill, 1985; Smith & March, 2001). Moreover, the fact that molecules carrying the C═S group tend to form hydrogen bonds shorter than the corresponding C═O derivatives (see CSD data of Table 2) can also be easily understood in terms of a better pK_a matching due to the increased acidic character of thioamides with respect to amides. This can be shown, for example, by the comparison of the pK_a values measured for acetamide and thioacetamide in DMSO, which are 25.5 (Bordwell *et al.*, 1978) and 18.5 (Bordwell & Ji, 1991), respectively. These considerations are in agreement with the finding (Ferretti *et al.*, 1993; Galabov *et al.*, 2003) that thioamides are systematically more π-delocalized than amides and, for this reason, exhibit higher energetic barrier to the rotation around the C—N bond (difference in energy up to 12.56–16.75 kJ mol^{-1}) than amides do.

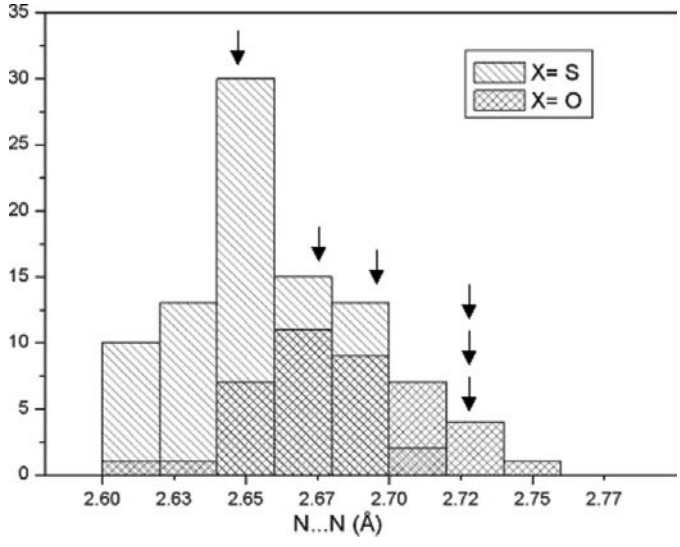

Figure 5
Histogram of N···N contact distances in molecules containing the fragment of Scheme (II). The arrows indicate the positions of N···N values found in the present molecules.

DFT calculations have been performed to evaluate the energetic contribution of the intramolecular hydrogen bond to the total energy of the molecules. Hydrogen-bond energies have been calculated as the energy difference, ΔE_{HB}, between the *open* and *closed* conformations of the sample molecules (*a*) and (*b*), as already described in §2. The DFT-calculated d_1–d_4 and hydrogen-bond structural parameters of the closed form are reported in the last two columns of Table 2. The optimized geometries are in reasonable agreement with the average experimental values of Table 2, even though the calculated N···N distances of 2.731 and 2.746 Å for (*a*) and (*b*), respectively, are somewhat longer than the experimental mean values. The evaluated ΔE_{HB} energies are very similar for the two sample molecules, being of 50.41 and 51.50 kJ mol^{-1} for (*a*) and (*b*), respectively.

These values can be compared with the energies of normal O—H···O bonds, *e.g.* 12.56–20.93 kJ mol^{-1} in water dimers (Curtiss & Blander, 1988), or with energies of strong O—H···O intramolecular RAHBs, which have been evaluated to be some 58.62–62.80 kJ mol^{-1} for beta-diketone enols (Gilli, Ferretti *et al.*, 1996). This comparison clearly indicates that the values of 50.24–54.43 kJ mol^{-1} found in the pseudo-RAHB (II) are considered to be very large and therefore suggest this pattern (II) is very efficient in strengthening the N—H···N bond. This leads us to a final consideration. The energetic gain due to the formation of this particular hydrogen bond is so high as to assure that such a bond is most probably maintained in solution, as proved by NMR and IR spectroscopic experimental evidences (Bertolasi *et al.*, 1997). In view of these results, it seems reasonable to form the hypothesis that triazolo-pyrazolo-pyrimidine derivatives containing the ureidic —NH—C(═O,S)—NH—C═N— fragment are recognized and bound by the adenosine receptors in their planar conformation, in contrast with what was reported in a recent study (Baraldi *et al.*, 2002) in which a molecule belonging to the same chemical class is docked to a model of the A_3 receptor interacting with it in its 'open' conformation.

References

Accelrys Inc. (2003). *MaterialStudio*, MS modeling Version 3.0. Accelrys Inc., 6985 Scranton Road, San Diego, CA 92121-3752, USA.

Allen, F. H., Bellard, S., Brice, M. D., Cartwright, B. A., Doubleday, A., Higgs, H., Hummelink, T., Hummelink-Peters, B. G., Kennard, O., Motherwell, W. D. S., Rodgers, J. & Watson, D. G. (1979). *Acta Cryst.* B**35**, 2331–2339.

Altomare, A., Burla, M. C., Camalli, M., Cascarano, G., Giacovazzo, C., Guagliardi, A., Moliterni, A. G., Polidori, G. & Spagna, R. (1999). *J. Appl. Cryst.* **32**, 115–121.

Baraldi, P. G., Cacciari, B., Borea, P. A., Varani, K., Pastorin, G., de Ros, T., Tabrizi, M. A., Fruttarolo, F. & Spalluto, G. (2002). *Curr. Pharm. Des.* **6**, 2299–2332.

Baraldi, P. G., Cacciari, B., Romagnoli, R., Spalluto, G., Moro, S., Klotz, K. N., Leung, E., Varani, K., Gessi, S., Merighi, S. & Borea, P. A. (2000). *J. Med. Chem.* **43**, 4768–4780.

Baraldi, P. G., Tabrizi, M. A., Preti, D., Bovero, A., Fruttarolo, F., Romagnoli, R., El-Kashef, H., Moorman, A., Varani, K., Gessi, S., Merighi, S. & Borea, P. A. (2003). *J. Med. Chem.* **46**, 1229–1241.

Baraldi, P. G., Tabrizi, M. A., Preti, D., Bovero, A., Fruttarolo, F., Romagnoli, R., Zaid, N. A, Moorman, A. R., Varani, K. & Borea, P. A. (2005). *J. Med. Chem.* **48**, 5001–5008.

Baraldi, P. G., Tabrizi, M. A., Preti, D., Bovero, A., Romagnoli, R., Fruttarolo, F., Zaid, N. A., Moorman, A. R., Varani, K., Gessi, S., Meriggi, S. & Borea, P. A. (2004). *J. Med. Chem.* **6**, 1434–1447.

Barone, V. & Adamo, C. (1996). *J. Chem. Phys.* **105**, 11007–11019.

Berk, B., Akgun, H., Erol, K., Sirmagul, B., Gao, Z. G & Jacobson, K. A. (2006). *Farmaco*, **60**, 974–980.

Bertolasi, V., Gilli, P., Ferretti, V. & Gilli, G. (1997). *J. Chem. Soc. Faraday Trans.* pp. 945–952.

Bordwell, F. G., Bartmess, J. E. & Hautala, J. A. (1978). *J. Org. Chem.* **43**, 3095–3101.

Bordwell, F. G. & Ji, G. Z. (1991). *J. Am. Chem. Soc.* **113**, 8398–8401.

Buemi, G. & Zuccarello, F. (1996). *J. Chem. Soc. Faraday Trans.* **92**, 347–351.

Burnett, M. N. & Johnson, C. K. (1996). *ORTEP*III. Report ORNL-6895. Oak Ridge National Laboratory, Oak Ridge, Tennessee, USA.

Chung, G., Kwon, O. & Kwon, Y. J. (1997). *J. Phys Chem. A*, **101**, 4628–4632.

Colotta, V., Catarzi, D., Varano, F., Cecchi, L., Filacchioni, G., Martini, C., Trincavelli, L. & Lucacchini, A. (2000). *J. Med. Chem.* **43**, 3118–3124.

Curtiss, L. A. & Blander, M. (1988). *Chem. Rev.* **88**, 827–841.

Farrugia, L. J. (1999). *J. Appl. Cryst.* **32**, 837–838.

Ferretti, V., Bertolasi, V., Gilli, P. & Gilli, G. (1993). *J. Phys. Chem.* **97**, 13568–13574.

Fossa, P., Pestarino, M., Menozzi, G., Mosti, L., Schenone, S., Ranize, A., Bondavilli, F., Trincavelli, M. L., Lucacchini, A. & Martini, C. (2005). *Org. Biomol. Chem.* **3**, 2262–2270.

Fredholm, B. B., Ijzerman, A. P., Jacobson, K. A., Klotz, K.-N. & Linden, J. (2001). *Pharm. Rev.* **53**, 527–552.

Frisch, M. J., Scheiner, A. C., Schaefer, H. F. III & Binkley, J. S. (1985). *J. Chem. Phys.* **82**, 4194–4198.

Galabov, B., Ilieva, S., Hadjieva, B. & Dinchova, E. (2003). *J. Phys. Chem. A*, **107**, 5854–5861.

Gao, Z.-G., Kim, S.-K., Biadatti, T., Chen, W., Lee, K., Barak, D., Kim, S. G., Johnson, C. R. & Jacobson, K. A. (2002). *J. Med. Chem.* **45**, 4471–4484.

Gilli, P., Bertolasi, V., Ferretti, V. & Gilli, G. (1994). *J. Am. Chem. Soc.* **116**, 909–915.

Gilli, P., Bertolasi, V., Ferretti, V. & Gilli, G. (2000). *J. Am. Chem. Soc.* **122**, 10405–10417.

Gilli, P., Bertolasi, V., Pretto, L., Antonov, L. & Gilli, G. (2005). *J. Am. Chem. Soc.* **127**, 4943–4953.

Gilli, P., Bertolasi, V., Pretto, L., Ferretti, V. & Gilli, G. (2004). *J. Am. Chem. Soc.* **126**, 3845–3855.

Gilli, P., Bertolasi, V., Pretto, L., Lycka, A. & Gilli, G. (2002). *J. Am. Chem. Soc.* **124**, 13554–13567.

Gilli, P., Fernàndez-Castaño, C., Ferretti, V. & Gilli, G. (1996). XXVI Congress of the Italian Association of Crystallography, Alessandria, Italy, p. 124.

Gilli, P., Ferretti, V., Bertolasi, V. & Gilli, G. (1996). *Advances in Molecule Structure Research*, edited by M. Hargittai & I. Hargittai, pp. 67–102. Greenwich, Connecticut, USA: JAI Press Inc.

Hayallah, A. M., Sandoval-Ramirez, J., Reith, U., Schobert, U., Preiss, B., Schumacher, B., Daly, J. W. & Mueller, C. E. (2002). *J. Med. Chem.* **45**, 1500–1510.

Hess, S., Mueller, C. E., Frobenius, W., Reith, U., Klotz, K.-N. & Eger, K. (2000). *J. Med. Chem.* **43**, 4636–4646.

Jacobson, K. A. (1998). *Trends Pharmacol. Sci.* **19**, 184–191.

Jarvis, M. F. & Williams, M. (1987). *Trends Pharmacol. Sci.* **8**, 330–332.

Kim, Y.-C., Ji, X., Melman, N., Linden, J. & Jacobson, K. A. (2000). *J. Med. Chem.* **43**, 1165–1172.

Kim, Y.-C., de Zwart, M., Chang, L., Moro, S., von Frijtag Drabbe Kunzel, J., Melman, N., Ijzerman, A. P. & Jacobson, K. A. (1998). *J. Med. Chem.* **41**, 2835–2845.

Kim, S., Marshall, M. A., Melman, N., Kim, H. S., Mueller, C. E., Linden, J. & Jacobson, K. A. (2002). *J. Med. Chem.* **45**, 2131–2138.
Kobko, N., Paraskevas, L., del Rio, E. & Dannenberg, J. J. (2001). *J. Am. Chem. Soc.* **123**, 4348–4349.
Maskill, H. (1985). *The Physical Basis of Organic Chemistry*. New York: Oxford University Press.
Müller, C. E. (1997). *Exp. Opin. Ther. Patents*, **5**, 419–440.
Nardelli, M. (1995). *J. Appl. Cryst.* **28**, 659–659.
Nonius (1997). *Kappa-CCD Server Software*. Nonius BV, Delft, The Netherlands.
Otwinowski, Z. & Minor, W. (1997). *Methods Enzymol.* **276**, 307–326.
Perdew, J. P. & Wang, Y. (1992). *Phys. Rev. B*, **45**, 13244–13249.
Richardson, P. J., Kase, H. & Jenner, P. G. (1997). *Trends Pharmacol. Sci.* **18**, 338–344.
Sheldrick, G. M. (1997). *SHELX*97. University of Göttingen, Germany.
Smith, M. B. & March, S. (2001). *Advanced Organic Chemistry*, 5th Ed. New York: J. Wiley and Sons.